

RESEARCH ARTICLE

Open Access



# Synthesis, spectral, thermal, crystal structure, Hirschfeld analysis of [*bis*(triamine) Cadmium(II)][Cadmium(IV)tetra-bromide] complexes and their thermolysis to CdO nanoparticles

Ismail Warad<sup>1\*</sup>, Fuad Al-Rimawi<sup>2</sup>, Assem Barakat<sup>3,4\*</sup>, Saida Affouneh<sup>5</sup>, Naveen Shivalingegowda<sup>6</sup>, Nartur Krishnappagowda Lokanath<sup>7</sup> and Ibrahim M. Abu-Reidah<sup>1</sup>

## Abstract

**Background:** The coordination chemistry of cadmium(II) with diamine ligands is of particular interest. The most common structure around cadmium(II) center in their complexes is tetrahedral, that is due the octet rule obeyed. Nevertheless, five and six-coordinated complexes are also well known. Now a day, many cadmium(II) complexes with chelate ligands were synthesized for their structural or applications properties. Antibacterial activities and DNA binding affinity of this class of cadmium complexes have attracted considerable interest.

**Results:** Cadmium(II) complexes in dicationic form with general formula  $[\text{Cd}(\text{dien})_2]\text{CdBr}_4$  complex **1** (dien = diethylenetriamine) and  $[\text{Cd}(\text{dipn})_2]\text{CdBr}_4$  complex **2** (dipn = diprolylenetriamine) were prepared and elucidated their chemical structures by elemental analysis, UV-Vis, IR, TG and NMR, additionally complex **1** structure was solved by X-ray diffraction study. The Cd(II) cation is located in a slightly distorted octahedral geometry while Cd(IV) anion is in tetrahedral geometry. High stability of the synthesized complexes confirmed by TG. Thermolysis of complex **1** revealed the formation of pure cubic nanoparticles CdO which was deduced by spectral analysis. The average size of CdO nanoparticles was found to be ~60 nm.

**Conclusions:** Two new Cd(II) complexes of general formula  $[\text{Cd}(\text{N}_3)_2]\text{CdBr}_4$  were made available. The structure of  $[\text{Cd}(\text{dien})_2]\text{CdBr}_4$  was confirmed by X-ray diffraction. Thermal, electro and spectral analysis were also investigated in this study. The direct thermolysis of such complexes formed a cubic CdO regular spherical nanoparticle with the ~60 nm average particle size.

**Keywords:** Cadmium(II) complexes, Triamine, XRD, CdO nanoparticles

## Background

Cadmium(II) complexes with polydentate nitrogen ligands, mainly polyamines, have been studied for some time either because of their structural properties [1, 2] or

their applications [3–7]. The synthesis and characterization of triamine complexes of transition and non-transition metals are of interest as they can potentially exist in three isomeric forms, i.e. mer and fac [8, 9]. The shape of cadmium(II) halide complex anions depending on the number of hydrogen bonds and the cations species [2–5]. There are variable shapes of the complex anions such as tetrahedral [10, 11], two-dimensional layered structures [12], and complex chain structures [13–15]. Cadmium complexes have attracted considerable interest due to

\*Correspondence: warad@najah.edu; ambarakat@ksu.edu.sa

<sup>1</sup> Department of Chemistry, Science College, An-Najah National University, P.O. Box 7, Nablus, Palestine

<sup>3</sup> Department of Chemistry, College of Science, King Saud University, P. O. Box 2455, Riyadh 11451, Saudi Arabia

Full list of author information is available at the end of the article

pharmacological importance including anti-microbial agents [4], DNA binding affinity [3], and anticancer activities [5–7, 16, 17].

The design and development of novel functional materials utilizing non-covalent interactions in complexes have attracted considerable attention [17–20]. Various weak dispersive interactions, such as hydrogen bonding and other weak interactions involving  $\pi$ -cloud of the aromatic ring represents the backbone of self-assembly process to stabilize the crystals [22]. Hydrogen bonding interactions are the most reliable and widely used in building multi-dimensional supramolecular structures [21–23].

In the last decade, spherical shape metal oxide nanoparticles [24] composed of a mixed-ligand dinuclear and mononuclear cadmium(II) complexes building blocks [25–28]. We reported the synthesis and characterization of two new dicationic cadmium(II) complexes with general formula  $[\text{Cd}(\text{N}_3)_2]\text{CdBr}_4$ . Complex **1** used as building block for preparation the CdO nanoparticles by direct open atmosphere thermolysis process.

## Results and discussion

### Synthesis of the desired complexes

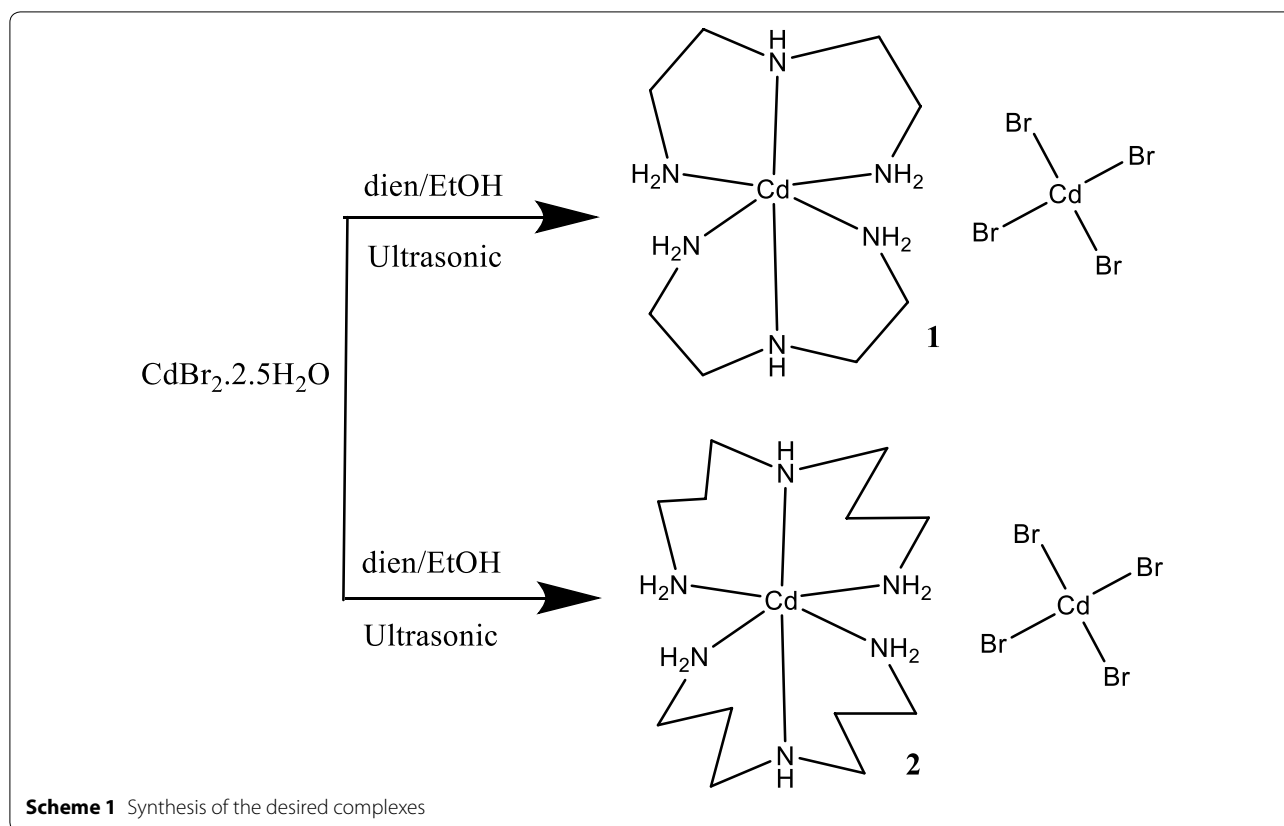
Two new dicationic Cd(II) complexes with general formula  $[\text{Cd}(\text{N}_3)_2]\text{CdBr}_4$  have been prepared by mixing of

excess of the tridentate free ligands with  $\text{CdBr}_2 \cdot 2.5\text{H}_2\text{O}$  in EtOH under open ultrasonic atmosphere. The dicationic Cd(II) complexes were prepared in very good yield without side products, as seen in Scheme 1.

The X-ray single crystal diffraction technique used to confirm the structure of the target complex **1** and other spectral analysis including elemental analysis, IR, UV-vis, TG/DTA, CV and NMR. The isolated complexes are stable in air, soluble only in water, DMF and DMSO. The dicationic nature was supported by high water solubility (0.02 g/ml at RT) and molar conductance ( $\Lambda_M = 190 \Omega^{-1}\text{cm}^2 \text{mol}^{-1}$  of  $1 \times 10^{-3}\text{M}$  at RT) showed that the two complexes are electrolytic in their nature. The analytical data of the  $[\text{Cd}(\text{dien})_2]\text{CdBr}_4$  desired complex consisted with XRD analysis data. The TG-residue product of complex **1** revealed the formation of CdO cubic nanoparticle [23]. The gentle heating with fixed heat of rate as well as the N6-tridentate ligands may play the critical role in de-structure of the desired complexes to CdO nanoparticles.

### X-ray crystal structure of complex **1**

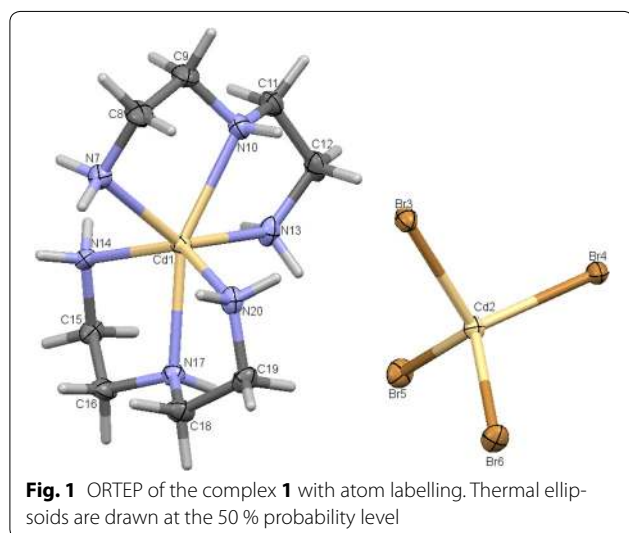
An asymmetric unit cell consists of two  $\text{Cd}^{2+}$  ions of which one is a cation and the other counter ion, two dien fully coordinated to the Cadmium cation center. An N6 coordinated complex is formed. The Cd(II) cation are



located in a slightly distorted octahedral geometry while Cd(IV) counter anion are in tetrahedral geometry seen in Fig. 1. The bond length between the Cd(IV) anions and the bromine atoms are in the expected range except for the elongation of Br3 atom which is actively involved in the hydrogen bonding as seen in Fig. 2. This type of hydrogen bonding helps in the better stabilization of the crystal structure. A study of torsion angles, asymmetric parameters and least-square plane calculations reveals that one of the four five membered ring the ring adopts an envelope conformation with the atoms N10 and N13 deviating 0.230 (3) and  $-0.109$  (3) Å respectively from the Cremer and Pople plane [29]. This is confirmed by the puckering parameters  $Q = 0.472$  (3) Å and  $\phi = 255.5$  (3). The other three five membered rings adopts a twisted conformation on the bonds C8–C9, C15–C16 and C18–C19 respectively. The structure exhibits both inter and intramolecular hydrogen bonds of the N–H...Br and C–H...Br which helps in stabilizing the crystal structure [14, 15]. Packing of the molecules when viewed down along the *a* axis indicates that the molecules exhibit layered stacking and several hydrogen bonds as seen in Fig. 3. The crystal data deposited and can be retrieved via CCDC 1404033.

#### IR spectrum

The IR spectrum of complex 1 is depicted in Fig. 4. Complex 1 revealed three main characteristic absorptions peaks in the range 3180–3300, 2780–2850 and 650–450  $\text{cm}^{-1}$ , which was assigned to N–H, C–H<sub>alkyl</sub> and Cd–N stretching vibrations, respectively [25–27]. No water was recorded in the structures of the complexes. The chemical shifts of N–H functional groups of dipen coordinated to the Cd(II) center in the complexes was



shifted down filed by  $\sim 60$   $\text{cm}^{-1}$  compared by the free one, this support the tridentate ligand full coordination to the Cd(II) center.

#### UV–Vis spectral study

The UV–Vis absorption spectra of the complex 1 and complex 2 in water solvent presented one sharp dominant bands at 270 and 280 nm respectively, no other bands were detected elsewhere, as seen in Fig. 5. The cadmium centers showed only the charge transfer transitions which can be assigned to charge transfer from the metal to ligand and vice versa ( $d-\sigma^*$  electron transfer), no absorption resonated to  $\pi-\pi^*$  electron transfer (dien and dipn ligands are saturated) or  $d-d$  transition are expected for  $d^{10}$  Cd(II) complexes [30, 31].

#### NMR investigation

The  $^1\text{H}$  and  $^{13}\text{C}\{^1\text{H}\}$  NMR spectra of the synthesized complexes were carried out in  $d^6$ -DMSO solvent to confirm the binding of the dien ligands to the cadmium(II) in 2–1 ration respectively. The  $^1\text{H}$  and  $^{13}\text{C}\{^1\text{H}\}$  NMR spectra corroborate the structure of the desired complexes as well as the XRD; only three functional groups,  $^1\text{H}$  NMR ( $d^6$ -DMSO): d (ppm) 2.55 and 2.62 (2 br, 16H, 8 $\text{CH}_2$ ), 2.85 (br, 8H, 4 $\text{NH}_2$ ), 3.35 (br, 2H, 2NH), signals belonging to the  $\text{CH}_2\text{CH}_2$  and  $\text{NH}_2$  of dien ligand coordinated with  $\text{CdBr}_2$  were recorded, as depicted in Fig. 6.

#### TG analysis

The TG of the complex was carried out in the range of 0–800  $^\circ\text{C}$  and 10  $^\circ\text{C}/\text{min}$  heating rate, typical thermal TG curve are given in Fig. 7 which shows that there is no coordinated or uncoordinated water in the range 0–180  $^\circ\text{C}$ . Also organic and inorganic contents were de-structured away (to  $\text{CO}_2$ ,  $\text{NO}_x$  gas product) from the Cd(II) metal center in one step decomposition in range 290–500  $^\circ\text{C}$  with  $\sim 80$  % weight loss. The final product (20 % residue) was confirmed to be CdO by IR [32–34].

#### CdO nanoparticle formed by direct thermolysis of complex 1

The phase information and composition of the TG final residue produced through open atmosphere thermolysis of complex 1 was deduced by FT-IR, X-ray powder diffraction (XRD), EDX, SEM and TEM. The product was characterized as CdO nanoparticles.

Figure 8 shows the IR spectrum product CdO nanoparticle, the formation of CdO nanoparticle was supported by two signs vibration at 420 and 560  $\text{cm}^{-1}$  belongs to Cd=O bond, it could be useful in understanding the bonding between the Cd–O atoms [32]. All the other vibration assigned to the starting complexes was disappeared due to the thermal digestion of all organic contents.

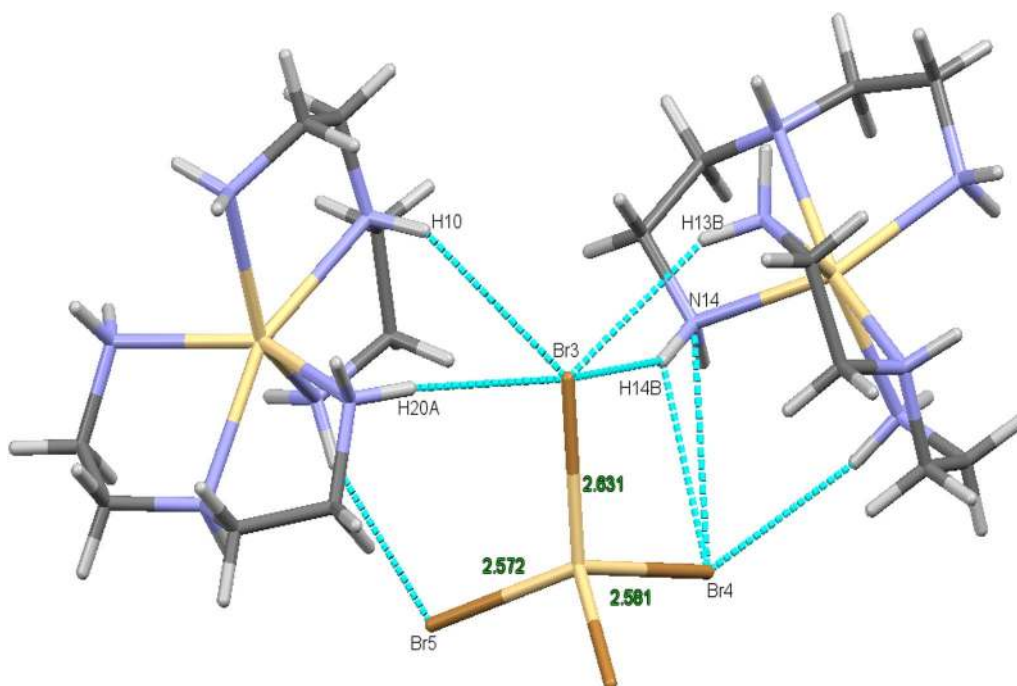


**Fig. 2** Elongation of bond length of Br3 atom due to hydrogen bonding. The *dotted lines* indicate hydrogen bonds

The (111), (200) and (220) reflections are closely match the reference CdO prepared with JCPDS file No. 05-0640, the formation of CdO cubic crystal nanoparticle was confirmed, see Fig. 9. The particles were found in polycrystalline structure and that the nanostructure grew in a random orientation which confirmed by sharp peaks from XRD data [32–36].

The size and morphology of these particles were determined by Scanning Electron Microscopy (SEM) before and after calcination, as seen in Fig. 10a, b, respectively. SEM image for complex 1, particles were irregular before calcination, while after calcination regular spherical particles were collected, which confirmed that tridentate organic ligands play de-structure role during thermolysis process [30–36]. According to this micrograph, nanoparticles with less than 100 nm in diameter were produced.

Also, TEM was carried out for the CdO nanoparticles corresponding to the same sample above was illustrated in Fig. 11. From TEM image, the average size of the nanoparticles found to be around 60 nm. The particles are spherical in shape, not unlike those reported by Dong et al. [34].

#### Hirshfeld surface analysis for complex 1

Crystal structure analysis of complex 1 using the cif file was generated by Hirshfeld Surface, to analysis the intermolecular interactions then illustrated the fingerprint map of atoms<sub>inside</sub>/atom<sub>outside</sub> interactions of

molecules. The Hirshfeld surfaces of complex 1 is displayed in Fig. 12, showing surfaces that have been mapped over a  $d_{\text{norm}}$ ,  $d_e$  and  $d_i$  [37, 38]. “For each point on that isosurface two distances are determined: one is  $d_e$  represents the distance from the point to the nearest nucleus external to the surface and second one is  $d_i$  represents the distance to the nearest nucleus internal to the surface. The dark-red spots on the  $d_{\text{norm}}$  surface arise as a result of the short interatomic contacts, i.e. strong hydrogen bonds, while the other intermolecular interactions appear as light-red spots [18–22]”. The surface here in this work represents the circular depressions (deep red) visible on the Hirshfeld surface indicative of strong hydrogen bonding contacts of types N–H...Br and C–H...Br.

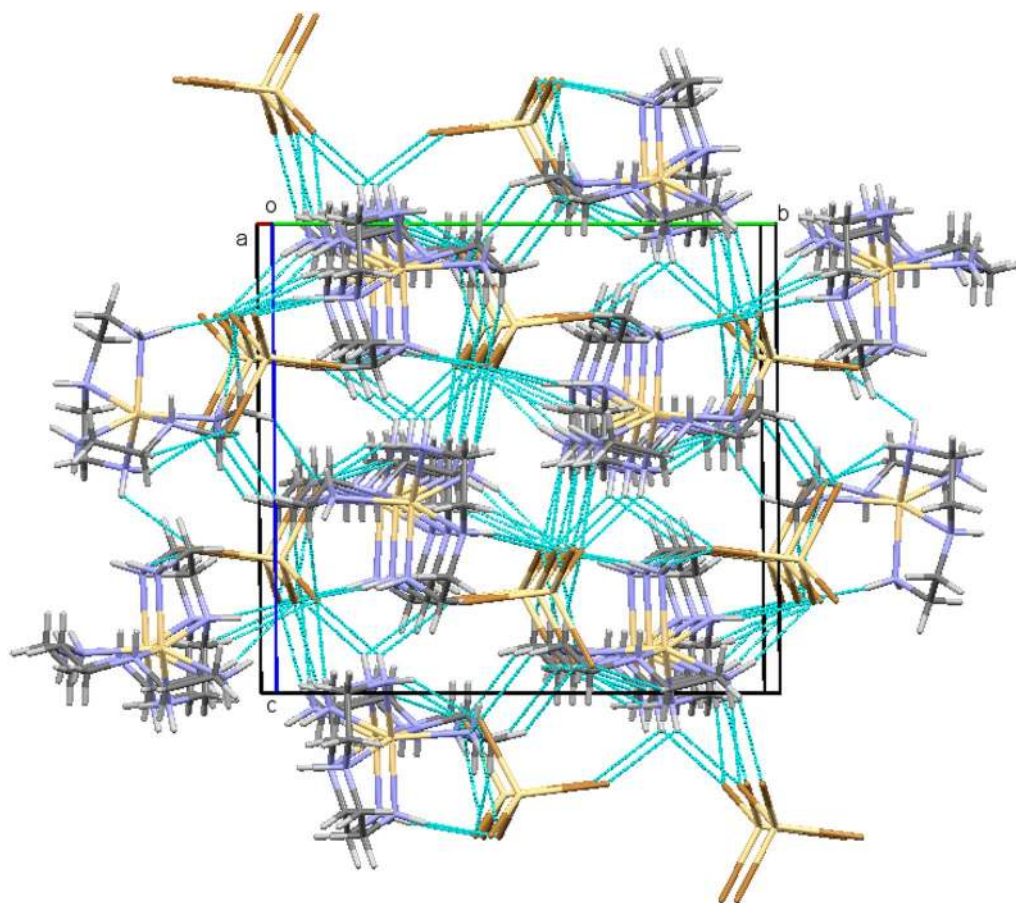
The two-dimensional fingerprint plots over the Hirshfeld surfaces of complex 1 illustrate the significant differences between the intermolecular interaction patterns. H...all (64.6 %), Br...all (34.4 %), Cd...all (0.6 %) and all...all (Fig. 13) and Table 1.

Table 1 illustrate the detail fingerprints intermolecular interaction between inside and outside atoms in both neighbor molecules.

#### Experimental section

##### Material and instrumentation

“Dien, dipn ligands and  $\text{CdBr}_2 \cdot 2.5\text{H}_2\text{O}$  were purchased from Fluka. Elemental analyses were carried out on an



**Fig. 3** A crystal packing of complex **1** exhibiting layered stacking when viewed (perspective) along the crystallographic *a* axis. The *dotted lines* indicate hydrogen bonds

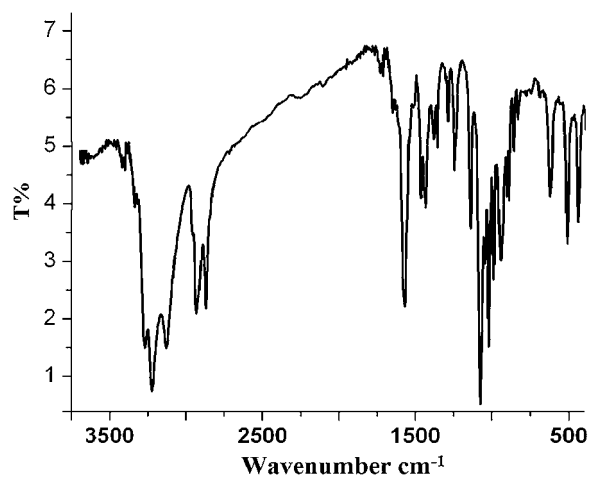


**Fig. 4** IR-KBr disk spectra of the complex **1**

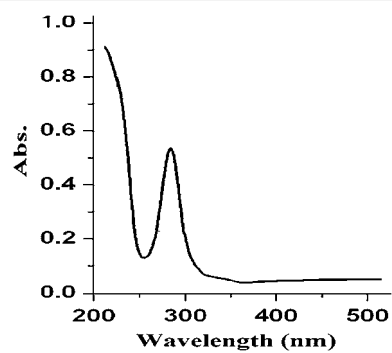
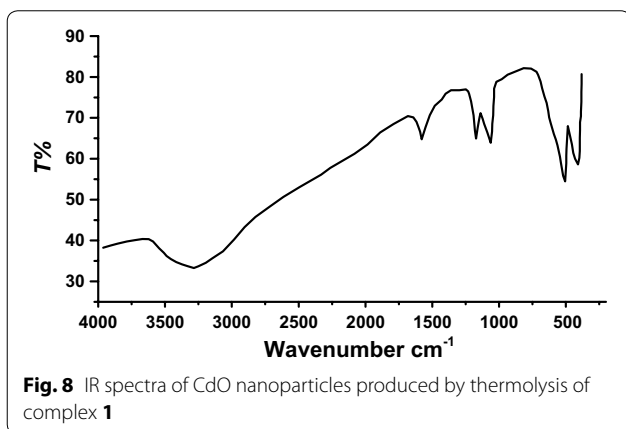
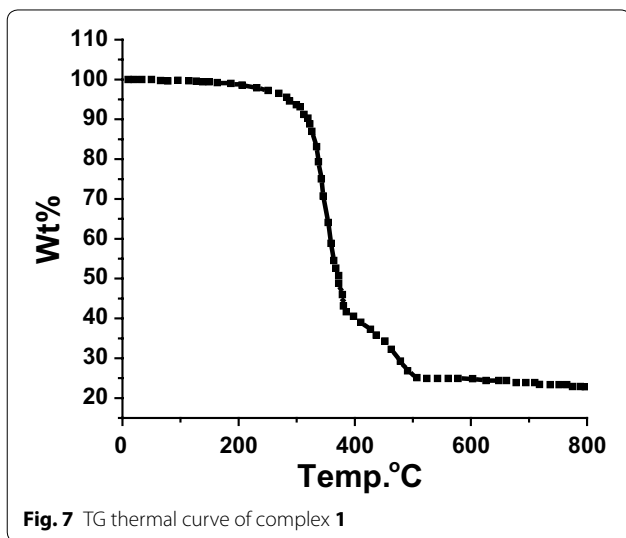
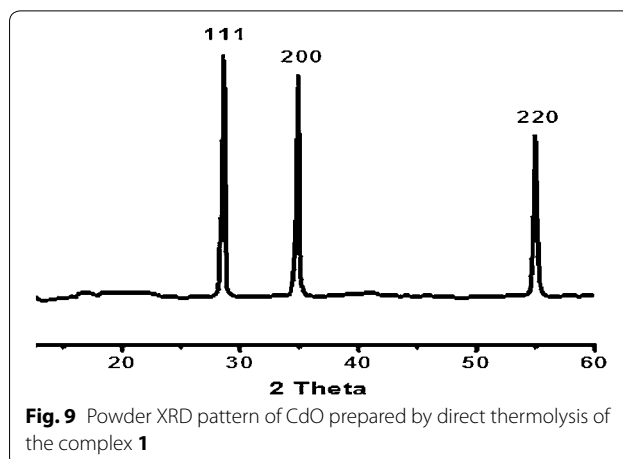
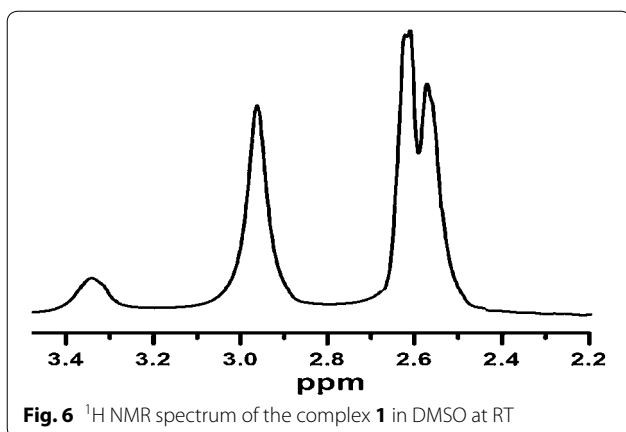


**Fig. 5** UV-Vis spectrum of the complex **1** in water at RT



ElementarVario EL analyzer. The IR spectra for samples were recorded using (Perkin Elmer Spectrum 1000 FT-IR Spectrometer). The UV-visible spectra were measured

by using a TU-1901 double-beam UV-visible spectrophotometer. TG/DTA spectra were measured by using a TGA-7 Perkin-Elmer thermogravimetric analyzer. The obtained nanoparticles were examined by a Bruker D/MAX 2500 X-ray diffractometer with Cu K radiation ( $\lambda = 1.54 \text{ \AA}$ ), and the operation voltage and current were maintained at 40 kV and 250 mA, respectively. The transmission electron microscopy (TEM, 1001 JEOL Japan). The scanning electron microscopy (SEM, JSM-6360 ASEM, JEOL Japan). The Hirshfeld surfaces analysis of complex **1** was carried out using the program CRYSTAL EXPLORER 3.1 [39].

#### General procedure for the preparation of the desired complexes

In an ultrasonic open atmosphere media, a mixture of  $\text{CdBr}_2 \cdot 2.5\text{H}_2\text{O}$  (2.0 mmol) in distilled ethanol (15 mL) and the free ligand was added in excess (6.0 mmol). The reaction mixture was subjected to ultrasonic vibration until the product complex appeared as white precipitate after ~20 min. The product was filtered and washed several times with ethanol. The product was only soluble in water, DMF and DMSO. Single crystals suitable for X-ray diffraction experiments were obtained by slow evaporation of water from complex solution.

#### Complex 1

Yield: (91 %). Anal. Calc. for  $\text{C}_8\text{H}_{26}\text{Br}_4\text{Cd}_2\text{N}_6$ : C, 12.80; H, 3.49; N, 11.19 %. Found. C, 12.53; H, 3.61; N, 11.28 %. MS  $[\text{M}^{+2}] = 320.0$  [theoretical = 320.2 m/z]. UV-Vis bands in water 275 nm. m.p 340 °C. Conductivity in DMF: 18.3 ( $\mu\text{S}/\text{cm}$ ).  $^1\text{H}$  NMR ( $d^6$ -DMSO): d (ppm) 2.55 and 2.62 (2br, 16H, 8 $\text{CH}_2$ ), 2.85 (br, 8H, 4 $\text{NH}_2$ ), 3.35 (br, 2H, 2NH),  $^{13}\text{C}\{^1\text{H}\}$  NMR ( $d^6$ -DMSO): d (ppm) 25.2 (s, 4C,  $\text{CH}_2$ ), 34.5 (s, 4C,  $\text{CH}_2$ ).

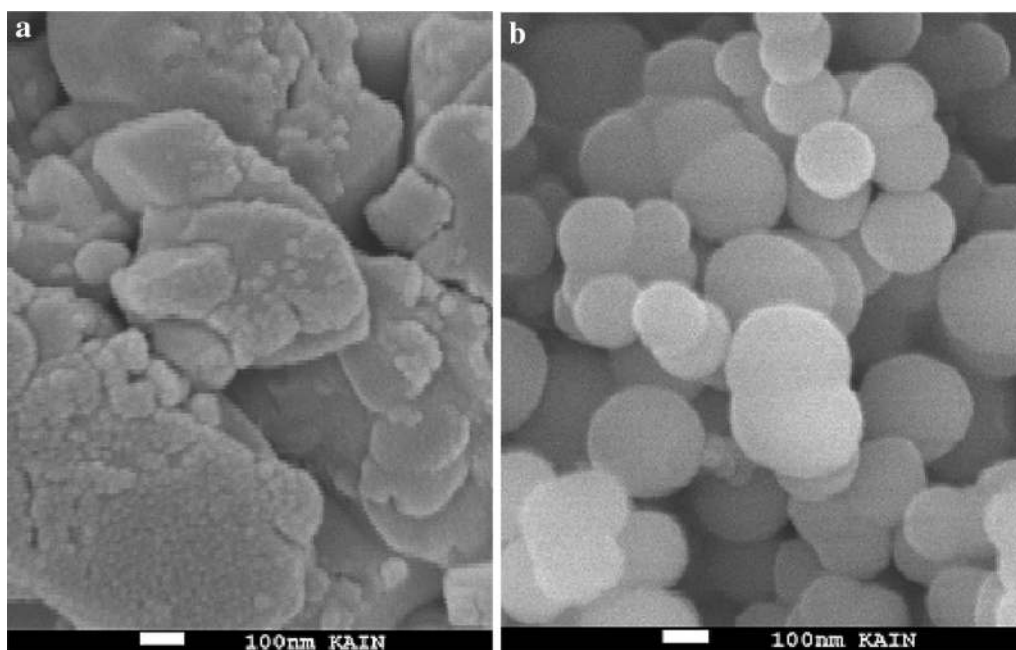


**Fig. 10** The SEM image of complex **1** **a** before and **b** after calcination to produce CdO nanoparticles

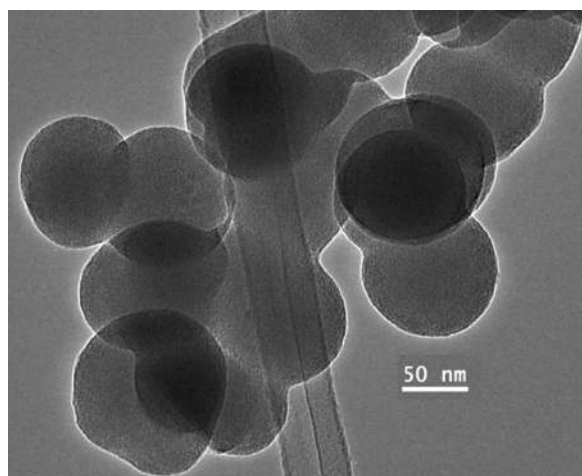


**Fig. 11** TEM image of CdO nanoparticles of an average diameter of ~60 nm

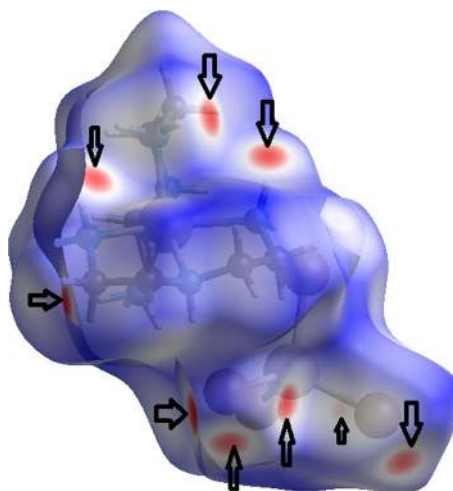


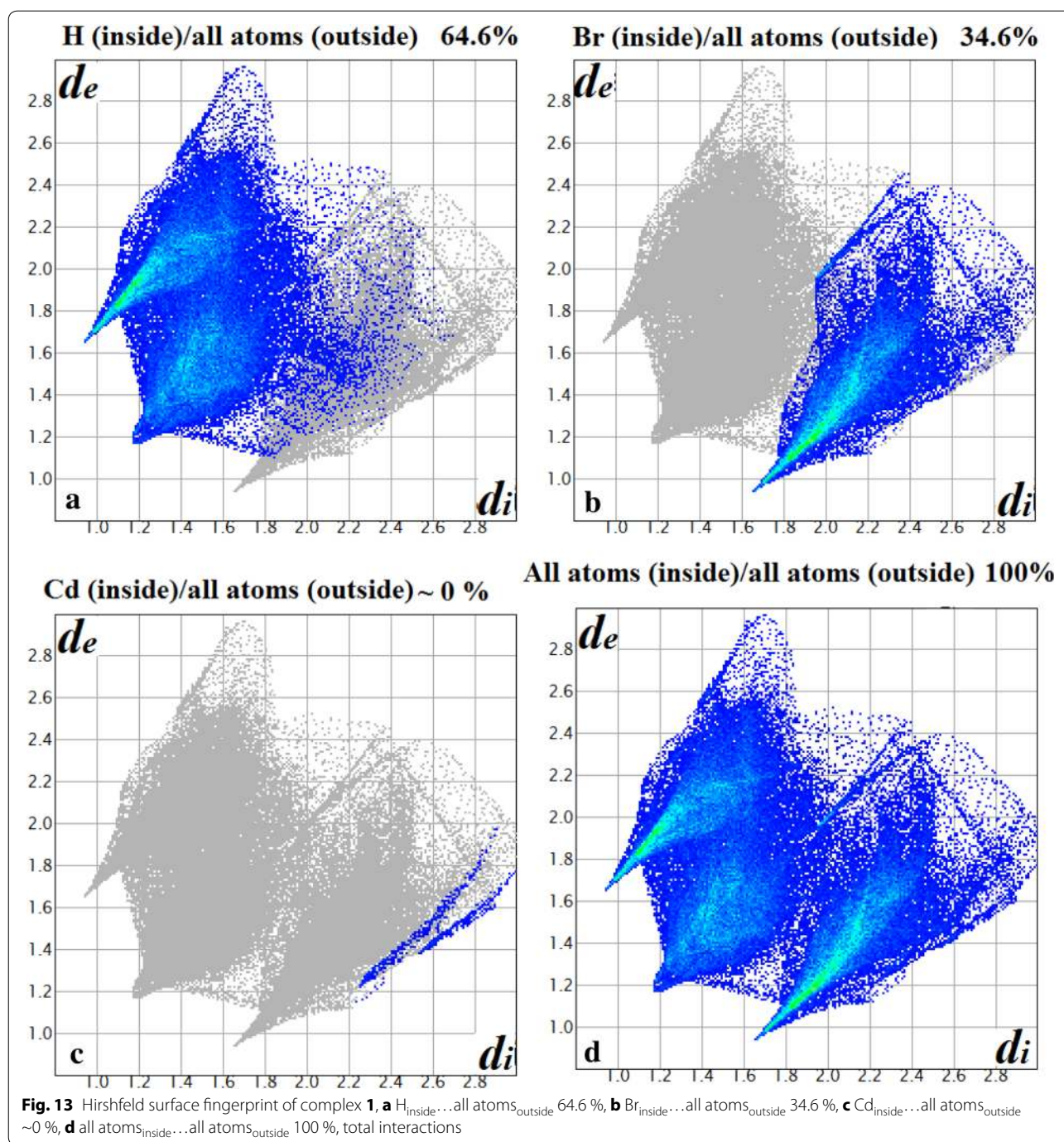
**Fig. 12**  $d_{norm}$  mapped on hirshfeld surface for visualizing the inter-contacts of complex **1**

### Complex 2

Yield: (88 %). Anal. Calc. for  $C_{12}H_{34}Br_4Cd_2N_6$ : C, 17.86; H, 4.25; N, 10.42 %. *Found.* C, 17.48; H, 4.21; N, 10.38 %. MS [ $M^{+2}$ ] = 376.0 [theoretical = 376.19 m/z]. UV-Vis bands in water 285 nm. m.p 320 °C. Conductivity in DMF: 22.3 ( $\mu S/cm$ ).  $^1H$  NMR ( $d^6$ -DMSO):  $\delta$  (ppm) 1.85 (br, 8H, 4CH<sub>2</sub>), 2.62 and 2.82 (2 br, 16H, 8CH<sub>2</sub>), 2.88 (br, 8H, 4NH<sub>2</sub>), 3.38 (br, 2H, 2NH),  $^{13}C\{^1H\}$  NMR ( $d^6$ -DMSO):  $\delta$  (ppm) 20.0 (s, 4C, CH<sub>2</sub>), 25.8 (s, 4C, CH<sub>2</sub>), 34.9 (s, 4C, CH<sub>2</sub>).

### Crystallography

A colourless prism shaped single crystal of dimensions  $0.35 \times 0.23 \times 0.19$  mm of the title compound was chosen for an X-ray diffraction study. The X-ray intensity Data were collected on a Bruker APEX-II CCD area diffractometer and equipped with graphite monochromatic MoK $\alpha$  radiation of wavelength 0.71073 Å at 100 (2) K. Cell refinement and data reduction were carried out using *SAINT PLUS* [24]. The structure was solved by direct methods and refined by full-matrix least



squares method on  $F^2$  using *SHELXS* and *SHELXL* programs [40]. All the non-hydrogen atoms were revealed in the first difference Fourier map itself. All the hydrogen atoms were positioned geometrically and refined using a riding model. After ten cycles of refinement, the final difference Fourier map showed peaks of no chemical significance and the residuals saturated to 0.0237. The geometrical calculations were carried out

using the program *PLATON* [41]. The molecular and packing diagrams were generated using the software *MERCURY* [42]. The details of the crystal structure and data refinement are given in Table 2. The list of bond lengths and bond angles of the non-hydrogen atoms are given in Table 3. Figure 6 represents the ORTEP of the molecule with thermal ellipsoids drawn at 50 % probability.



**Table 1 Inside/outside intermolecular interaction percentage by atoms**

100 %	H <sub>inside</sub>	Br <sub>inside</sub>	Cd <sub>inside</sub>	N <sub>inside</sub>	C <sub>inside</sub>
H <sub>outside</sub>	41.7	32.7	0	0	0
Br <sub>outside</sub>	22.4	0.8	0	0	0
Cd <sub>outside</sub>	0.2	0	0	0	0
N <sub>outside</sub>	0	0	0	0	0
C <sub>outside</sub>	0	0	0	0	0

**Table 2 Crystal data and structure refinement for Ligand and complex 1**

Parameter	Value
Empirical formula	C <sub>8</sub> H <sub>26</sub> Br <sub>4</sub> Cd <sub>2</sub> N <sub>6</sub>
Formula weight	750.79
Temperature	100 (2) K
Wavelength	0.71073 Å
Crystal system, space group	Monoclinic, <i>P21/n</i>
Unit cell dimensions	<i>a</i> = 9.4335 (12) Å <i>b</i> = 14.7512 (18) Å <i>c</i> = 14.7815 (18) Å $\beta$ = 100.131 (2)°
Volume	2024.9 (4) Å <sup>3</sup>
Z, calculated density	4, 2.463 Mg/m <sup>3</sup>
Absorption coefficient	9.993 mm <sup>-1</sup>
<i>F</i> <sub>(000)</sub>	1408
Crystal size	0.35 × 0.23 × 0.19 mm
Theta range for data collection	1.97–28.28°
Limiting indices	−12 ≤ <i>h</i> ≤ 12, 0 ≤ <i>k</i> ≤ 19, 0 ≤ <i>l</i> ≤ 19
Reflections collected/unique	4969/4960 [R(int) = 0.0000]
Refinement method	Full-matrix least-squares on <i>F</i> <sup>2</sup>
Data/restraints/parameters	4969/0/181
Goodness-of-fit on <i>F</i> <sup>2</sup>	1.057
Final R indices [ <i>I</i> > 2σ( <i>I</i> )]	<i>R</i> 1 = 0.0237, <i>wR</i> 2 = 0.0468
R indices (all data)	<i>R</i> 1 = 0.0328, <i>wR</i> 2 = 0.0494
Largest diff. peak and hole	0.595 and −0.885 e. Å <sup>-3</sup>

## Conclusions

For the first time, two new complexes [Cd(dien)<sub>2</sub>]CdBr<sub>4</sub> and [Cd(dipn)<sub>2</sub>]CdBr<sub>4</sub> were synthesized in good yield. The chemical structure of [Cd(dien)<sub>2</sub>]CdBr<sub>4</sub> was confirmed by X-ray diffraction. The Cd(II) cation center are located in a slightly distorted octahedral geometry while Cd(IV) anion are in tetrahedral and in high stability. Thermolysis of the complexes revealed the formation of CdO cubic nanoparticle, which was deduced by XRD, FT-IR, TEM and SEM, the average size of CdO nanoparticles found to be 60 nm.

**Table 3 Selected bond distances (Å) and bond angles (°) of complex 1**

Atoms	Length	Atoms	Length
Cd1-N14	2.346 (2)	C12-N13	1.472 (4)
Cd1-N20	2.357 (2)	N14-C15	1.475 (4)
Cd1-N7	2.365 (3)	C15-C16	1.516 (4)
Cd1-N13	2.365 (3)	C16-N17	1.469 (4)
Cd1-N17	2.410 (2)	N17-C18	1.471 (4)
Cd1-N10	2.422 (3)	C18-C19	1.512 (4)
N7-C8	1.474 (4)	C19-N20	1.476 (4)
C8-C9	1.517 (5)	Cd2-Br5	2.5721 (5)
C9-N10	1.463 (4)	Cd2-Br4	2.5809 (5)
N10-C11	1.468 (4)	Cd2-Br6	2.5835 (4)
C11-C12	1.514 (5)	Cd2-Br3	2.6313 (5)
Atoms	Angle	Atoms	Angle
N14-Cd1-N20	141.05 (9)	C11-N10-Cd1	107.43 (19)
N14-Cd1-N7	88.75 (9)	N10-C11-C12	109.8 (3)
N20-Cd1-N7	90.10 (9)	N13-C12-C11	110.7 (3)
N14-Cd1-N13	91.91 (9)	C12-N13-Cd1	111.76 (19)
N20-Cd1-N13	111.72 (9)	C15-N14-Cd1	108.88 (18)
N7-Cd1-N13	142.31 (9)	N14-C15-C16	109.2 (3)
N14-Cd1-N17	74.73 (8)	N17-C16-C15	110.1 (3)
N20-Cd1-N17	74.29 (9)	C16-N17-C18	114.7 (2)
N7-Cd1-N17	125.05 (9)	C16-N17-Cd1	107.94 (18)
N13-Cd1-N17	91.21 (9)	C18-N17-Cd1	107.01 (18)
N14-Cd1-N10	121.49 (9)	N17-C18-C19	109.7 (3)
N20-Cd1-N10	95.39 (9)	N20-C19-C18	109.4 (3)
N7-Cd1-N10	73.99 (9)	C19-N20-Cd1	110.46 (18)
N13-Cd1-N10	73.68 (9)	Br5-Cd2-Br4	109.305 (14)
N17-Cd1-N10	157.38 (9)	Br5-Cd2-Br6	108.258 (14)
C8-N7-Cd1	110.03 (19)	Br4-Cd2-Br6	111.585 (14)
N7-C8-C9	109.8 (3)	Br5-Cd2-Br3	111.083 (13)
N10-C9-C8	110.6 (3)	Br4-Cd2-Br3	104.874 (13)
C9-N10-C11	114.8 (3)	Br6-Cd2-Br3	111.720 (16)
C9-N10-Cd1	108.82 (19)		

## Supplementary material

Crystallographic data for complex **1** has been deposited with the Cambridge Crystallographic Data Centre as supplementary publication number CCDC 1404033. “Copies of this information may be obtained free of charge via <http://www.ccdc.cam.ac.uk/conts/retrieving.html> (or from the CCDC, 12 Union Road, Cambridge CB2 1EZ, UK; fax: +44-1223-336033; e-mail: [deposit@ccdc.cam.ac.uk](mailto:deposit@ccdc.cam.ac.uk))”.

## Authors' contributions

IW developed the synthesis, IW and IMA, undertook synthesis. FA help in analysis and interpretation of data collected and involved in drafting of manuscript. AB carried out some physical measurements. SA revision of draft for important intellectual content. NS and NK carried out the X-ray diffraction

measurement and help in writing the manuscript. All authors read and approved the final manuscript.

#### Author details

<sup>1</sup> Department of Chemistry, Science College, An-Najah National University, P.O. Box 7, Nablus, Palestine. <sup>2</sup> Chemistry Department, Faculty of Science and Technology, Al-Quds University, P.O. Box 20002, Al-Quds, Palestine. <sup>3</sup> Department of Chemistry, College of Science, King Saud University, P. O. Box 2455, Riyadh 11451, Saudi Arabia. <sup>4</sup> Department of Chemistry, Faculty of Science, Alexandria University, Ibrahimia, P.O. Box 426, Alexandria 21321, Egypt. <sup>5</sup> Elearning Center, An-Najah National University, P.O. Box 7, Nablus, Palestine. <sup>6</sup> Institution of Excellence, VijnanaBhavan, University of Mysore, Manasagangotri, Mysore 570 006, India. <sup>7</sup> Department of Studies in Physics, University of Mysore, Manasagangotri, Mysore 570 006, India.

#### Acknowledgements

The authors would like to extend their sincere appreciation to the Dean-ship of Scientific Research at King Saud University for its funding this Research group NO (RGP-257-2015).

#### Competing interests

The authors declare that they have no competing interests.

Received: 17 March 2016 Accepted: 18 May 2016

Published online: 13 June 2016

#### References

- Mitzi DB (2001) Templating and structural engineering in organic-inorganic perovskites. *J Chem Soc Dalton Trans* 1:1–12
- Martinez-Manez R, Sancenon F, Bijiyal M, Hecht M, Rurack K (2011) Mimicking tricks from nature with sensory organic-inorganic hybrid materials. *J Mater Chem* 21:12588–12604
- Rakibuddin M, Gazi S, Ananthkrishnan R (2015) Iron (II) phenanthroline-resin hybrid as a visible light-driven heterogeneous catalyst for green oxidative degradation of organic dye. *Catal Commun* 58:53–58
- Schoch TK, Hubbard JL, Zoch CR, Yi GB, Sørli M (1996) Synthesis and structure of the ruthenium (II) complexes  $[(\eta\text{-C5Me5})\text{Ru}(\text{NO})(\text{bipy})]^{2+}$  and  $[(\eta\text{-C5Me5})\text{Ru}(\text{NO})(\text{dppz})]^{2+}$ . DNA cleavage by an organometallic dppz Complex (bipy = 2, 2'-bipyridine; dppz = dipyrrodo [3, 2-a: 2', 3'-c] phenazine). *Inorg Chem* 35:4383–4390
- Kelland LR (2005) Overcoming the immortality of tumour cells by telomere and telomerase based cancer therapeutics—current status and future prospects. *Eur J Cancer* 41:971–979
- Song YM, Lu XL, Yang ML, Zheng XR (2005) Study on the interaction of platinum(IV), gold(III) and silver(I) ions with DNA. *Transit Metal Chem* 30:499–502
- Zhang QL, Liu JG, Chao H, Xue GQ, Ji LN (2001) DNA-binding and photocleavage studies of cobalt(III) polypyridyl complexes:  $[\text{Co}(\text{phen})_2\text{IP}]^{3+}$  and  $[\text{Co}(\text{phen})_2\text{PIP}]^{3+}$ . *J Inorg Biochem* 83:49–55
- Searle GH, House DA (1987) Lichens and fungi. XVIII. Extractives from *Pseudocyphellaria* rubella. *Aust J Chem* 40:361–372
- Cannas M, Marongiu G, Saba G (1980) Structures of the complexes of  $\text{CdCl}_2$  with the aliphatic triamines bis(2-aminoethyl)amine, bis(3-amino-propyl)amine, and 2-aminoethyl-(3-aminopropyl) amine: influence of aliphatic chain length on molecular association. *J Chem Soc Dalton Trans* 11:2090–2094
- Ishihara H, Dou SQ, Horiuchi K, Krishnan VG, Paulus H, Fuess H, Weiss A (1996) Isolated versus condensed anion structure: the influence of the cation size and hydrogen bond on structure and phase transition in  $\text{MX}_4^{2-}$  complex salts. 2,2-Dimethyl-1,3-propanediammonium tetrabromocadm(II) monohydrate, DimethylammoniumTetrabromozincate(II), and DimethylammoniumTetrabromocadm(II). *Z Naturforsch* 51a:1027–1036
- Ishihara H, Horiuchi K, Dou SQ, Gesing TM, Buhl JC, Paulus H, Fuess H (1998) Isolated versus condensed anion structure IV: an NQR study and x-ray structure analysis of  $[\text{H}_3\text{N}(\text{CH}_2)_3\text{NH}_3]\text{CdI}_4 \cdot 2\text{H}_2\text{O}$ ,  $[\text{H}_3\text{CNH}_2(\text{CH}_2)_3\text{NH}_3]\text{CdBr}_4$ ,  $[(\text{CH}_3)_4\text{N}]\text{CdBr}_4$ , and  $[(\text{CH}_3)_3\text{S}]\text{CdBr}_4$ . *Z Naturforsch* 53a:717–724
- Ishihara H, Krishnan VG, Dou SQ, Weiss A (1994) Bromine NQR and crystal structures of TetraaniliniumDecabromotricadm(II) and 4-methylpyridinium tribromocadm(II). *Z Naturforsch* 49a:213–222
- Ishihara H, Krishnan K, Dou SQ, Gesing TM, Buhl JC, Paulus H, Svoboda I, Fuess H (1999) Isolated versus condensed anion structure V: x-ray structure analysis and  $^{81}\text{Br}$  NQR of t-butylammoniumtribromocadm(II)-1/2 water, i-propylammoniumtribromocadm(II), and tris-trimethylammoniumheptabromocadm(II). *Z Naturforsch* 54a:628–636
- Ishihara H, Horiuchi K, Krishnan VG, Svoboda I, Fuess H (2000) Isolated versus condensed anion structure VI: x-ray structure analysis and  $^{81}\text{Br}$  NQR of GuanidiniumPentabromocadm(II),  $[\text{Cd}(\text{NH}_2)_3]\text{Cd}_2\text{Br}_5$ , tris-HydraziniumPentabromocadm(II),  $[\text{H}_2\text{NNH}_3]\text{CdBr}_5$ , and bis-HydraziniumTetrabromocadm(II)-tetra hydrate,  $[\text{H}_2\text{NNH}_3]_2\text{CdBr}_4 \cdot 4\text{H}_2\text{O}$ . *Z Naturforsch* 55a:390–396
- Ishihara H, Dou SQ, Horiuchi K, Krishnan VG, Paulus H, Fuess H, Weiss A (1996) Isolated versus condensed anion structure II; the influence of the cations (1,3-propanediammonium, 1,4-phenyldiammonium, and n-propylammonium) on structures and phase transitions of  $\text{CdBr}_4^{2-}$  salts A  $^{79,81}\text{Br}$  NQR and x-ray structure analysis. *Z Naturforsch* 51a:1216–1228
- Hines CC, Reichert WM, Griffin ST, Bond AH, Snowwhite PE, Rogers RD (2006) Exploring control of cadmium halide coordination polymers via control of cadmium (II) coordination sites utilizing short multidentate ligands. *J Mol Struct* 796(1):76–85
- He Y, Cai C (2011) Polymer-supported macrocyclic Schiff base palladium complex: an efficient and reusable catalyst for Suzuki cross-coupling reaction under ambient condition. *Cat Commun* 12(7):678–683
- Seth KS (2016) Tuning the formation of MOFs by pH influence: x-ray structural variations and hirshfeld surface analyses of 2-amino-5-nitropyridine with cadmium chloride. *CrystEngComm* 15:1772–1781
- Seth KS, Sarkar D, Kar T (2011) Use of  $\pi\text{-}\pi$  forces to steer the assembly of chromone derivatives into hydrogen bonded supramolecular layers: crystal structures and hirshfeld surface analyses. *CrystEngComm* 13:4528–4535
- Seth KS (2014) Discrete cubic water cluster: an unusual building block of 3D supramolecular network. *Inorg Chem Commun* 43:60–63
- Seth KS (2014) Exploration of supramolecular layer and bi-layer architecture in M(II)-PPP complexes: structural elucidation and hirshfeld surface analysis [PPP = 4-(3-Phenylpropyl)pyridine, M = Cu(II), Ni(II)]. *J Mol Struct* 1070:65–74
- Seth KS, Saha I, Estarellas C, Frontera A, Kar T, Mukhopadhyay S (2011) Supramolecular self-assembly of M-IDA complexes involving lone-pair- $\pi$  interactions: crystal structures, hirshfeld surface analysis, and DFT calculations  $[\text{H}_2\text{IDA} = \text{iminodiacetic acid}, \text{M} = \text{Cu}(\text{II}), \text{Ni}(\text{II})]$ . *Cryst Growth Des* 11:3250–3265
- Warad I, Khan AA, Azam M, Al-Resayes SI, Haddad SF (2014) Design and structural studies of diimine/ $\text{CdX}_2$  (X = Cl, I) complexes based on 2, 2-dimethyl-1, 3-diaminopropane ligand. *J Mol Struct* 1062:167–173
- Warad I, Azam M, Al-Resayes SI, Khan MS, Ahmad P, Al-Nuri M, Jodeh Sh, Husein A, Haddad SF, Hammouti B, Al-Noaimi M (2014) Structural studies on Cd(II) complexes incorporating di-2-pyridyl ligand and the X-ray crystal structure of the chloroform solvated DPMNPH/ $\text{CdI}_2$  complex. *Inorg Chem Commun* 43:155–161
- Warad I, Al-Ali M, Hammouti B, Hadda TB, Shareiah R, Rzaigui M (2013) Novel di- $\mu$ -chloro-bis [chloro (4, 7-dimethyl-1,10-phenanthroline) cadmium(II)] dimer complex: synthesis, spectral, thermal, and crystal structure studies. *Res Chem Intermed* 39:2451–2461
- Barakat A, Al-Noaimi M, Suleiman M, Aldwayyan AS, Hammouti B, Hadda TB, Haddad SF, Boshala A, Warad I (2013) One step synthesis of NiO nanoparticles via solid-state thermal decomposition at low-temperature of novel aqua (2, 9-dimethyl-1, 10-phenanthroline)  $\text{NiCl}_2$  complex. *Int J Mol Sci* 14:23941–23954
- Aldwayyan A, Al-Jekhedab F, Al-Noaimi M, Hammouti B, Hadda TB, Suleiman M, Warad I (2013) Synthesis and characterization of CdO nanoparticles starting from organometallic dmphen- $\text{CdI}_2$  complex. *Int J Electrochem Sci* 8:10506–10514
- Macrae CF, Bruno IJ, Chisholm JA, Edgington PR, McCabe P, Pidcock E, Rodriguez-Monge L, Taylor R, Van de Streek J, Wood PA (2008) Mercury CSD 2.0—new features for the visualization and investigation of crystal structures. *J Appl Cryst* 41:466–470
- Cremer DT, Pople JA (1975) General definition of ring puckering coordinates. *J Am Chem Soc* 97:1354–1358

30. Saghatforoush L, Aminkhani A, Ershad S, Karimnezhad GH, Ghammamy SH, Kabiri R (2008) Preparation of zinc (II) and cadmium (II) complexes of the tetradentate schiff base ligand 2-((E)-(2-(2-(pyridine-2-yl)-ethylthio)ethylimino)methyl)-4-bromophenol (PytBrsalH). *Molecules* 13:804–811
31. Majumder A, Rosair GM, Mallick A, Chattopadhyay N, Mitra S (2006) Synthesis, structures and fluorescence of nickel, zinc and cadmium complexes with the N, N, O-tridentate Schiff base N-2-pyridylmethylidene-2-hydroxy-phenylamine. *Polyhedron* 25:1753–1762
32. Warad I, Abdoh M, Shivalingegowda N, Lokanath NK, Salghi R, Al-Nuri M, Jodeh Sh, Radi S, Hammouti B (2015) Synthesis, spectral, electrochemical, crystal structure studies of two novel di- $\mu$ -halo-bis[halo (2, 9-dimethyl-4, 7-diphenyl-1, 10-phenanthroline) cadmium(II)] dimer complexes and their thermolysis to nanometal oxides. *J Mol Struct* 1099:323–329
33. Ye XR, Daraio C, Wang C, Talbot JB (2006) Room temperature solvent-free. Synthesis of monodisperse magnetite nanocrystals. *J Nanosci Nanotechnol* 6:852–856
34. Dong W, Zhu CS (2003) Optical properties of surface-modified CdO nanoparticles. *Opt Mater* 22(3):227–233
35. Klug HP, Alexander LE (1954) X-ray diffraction procedures for polycrystalline and amorphous materials. Wiley, New York
36. Patel RN, Singh N, Shukla KK, Niclós-Gutiérrez J, Castineiras A, Vaidyanathan VG, Nair BU (2005) Characterization and biological activities of two copper(II) complexes with diethylenetriamine and 2,2-bipyridine or 1,10-phenanthroline as ligands. *Spectrochim Acta Part A* 62:261–268
37. Spackman MA, Jayatilaka D (2009) Design and understanding of solid-state and crystalline materials. *Cryst Eng Commun* 11:19–32
38. Spackman MA, McKinnon JJ (2002) Fingerprinting intermolecular interactions in molecular crystals. *Cryst Eng Commun* 4:378–392
39. Wolff SK, Grimwood DJ, McKinnon JJ, Jayatilaka D, Spackman MA (2007) Crystal explorer 2.1. University of Western Australia, Perth
40. Bruker (2009) APEX2, SAINT and SADABS. Bruker AXS Inc, Madison
41. Sheldrick GM (2008) A short history of SHELX. *Acta Cryst A* 64:112–122
42. Spek AL (2009) Structure validation in chemical crystallography. *Acta Cryst D* 65:148–155

Submit your manuscript to a SpringerOpen<sup>®</sup> journal and benefit from:

- Convenient online submission
- Rigorous peer review
- Immediate publication on acceptance
- Open access: articles freely available online
- High visibility within the field
- Retaining the copyright to your article

---

Submit your next manuscript at ► [springeropen.com](http://springeropen.com)

---